HHS Public Access

Author manuscript

Biomaterials. Author manuscript; available in PMC 2016 December 01.

Published in final edited form as:

Biomaterials. 2015 December ; 71: 158–167. doi:10.1016/j.biomaterials.2015.08.042.

Ductile electroactive biodegradable hyperbranched polylactide copolymers enhancing myoblast differentiation

Meihua Xie[a], **Ling Wang**[a], **Baolin Guo**[a,*], **Zhong Wang**[b], **Y. Eugene Chen**[b], and **Peter X. Ma**[a,c,d,e,f,*]

[a]Center for Biomedical Engineering and Regenerative Medicine, Frontier Institute of Science and Technology, Xi'an Jiaotong University, Xi'an, 710049, China

[b]Department of Cardiac Surgery, Cardiovascular Center, The University of Michigan, Ann Arbor, MI 48109, USA

[c]Department of Biomedical Engineering, University of Michigan, Ann Arbor, MI 48109, USA

[d]Department of Biologic and Materials Sciences, University of Michigan, 1011, North University Ave., Room 2209, Ann Arbor, MI 48109, USA

[e]Macromolecular Science and Engineering Center, University of Michigan, Ann Arbor, MI 48109, USA

[f]Department of Materials Science and Engineering, University of Michigan, Ann Arbor, MI 48109, USA

Abstract

Myotube formation is crucial to restoring muscular functions, and biomaterials that enhance the myoblast differentiation into myotubes are highly desirable for muscular repair. Here, we report the synthesis of electroactive, ductile, and degradable copolymers and their application in enhancing the differentiation of myoblasts to myotubes. A hyperbranched ductile polylactide (HPLA) was synthesized and then copolymerized with aniline tetramer (AT) to produce a series of electroactive, ductile and degradable copolymers (HPLAAT). The HPLA and HPLAAT showed excellent ductility with strain to failure from 158.9% to 42.7% and modulus from 265.2 to 758.2 MPa. The high electroactivity of the HPLAAT was confirmed by UV spectrometer and cyclic voltammogram measurements. These HPLAAT polymers also showed improved thermal stability and controlled biodegradation rate compared to HPLA. Importantly, when applying these polymers for myotube formation, the HPLAAT significantly improved the proliferation of C2C12 myoblasts in vitro compared to HPLA. Furthermore, these polymers greatly promoted myogenic differentiation of C2C12 cells as measured by quantitative analysis of myotube number, length,

*To whom correspondence should be addressed: Peter X. Ma: mapx@umich.edu, Tel: +1 734-764-2209, Fax: +1 734-647-2805, Baolin Guo: baoling@mail.xjtu.edu.cn.

Supplementary data

Supporting information associated with this article can be found at http://www.journals.elsevier.com/biomaterials/.

diameter, maturation index, and gene expression of MyoD and TNNT. Together, our study shows that these electroactive, ductile and degradable HPLAAT copolymers represent significantly improved biomaterials for muscle tissue engineering compared to HPLA.

Keywords

degradable conducting polymers; ductile electroactive copolymer; polylactide; skeletal muscle regeneration; aniline oligomer

1. Introduction

Skeletal muscle tissue controls the voluntary movement and maintains the structural contour of the body. This soft tissue can be injured by toxic chemicals, biological factors, and physical destructions. Effective skeletal muscle tissue repair strategies are in high demand to improve the quality of such patients' life. Skeletal muscle tissue engineering represents such a strategy to overcome the disadvantages of transplanting host muscle tissue, such as donor site morbidity, long operative time, and poor rehabilitation [1]. Skeletal muscle tissue engineering often involves the prefabrication of muscle tissue in vitro by differentiation and maturation of muscle precursor cells on a scaffold, which provides the environmental conditions to facilitate the myogenic differentiation of the seeded cells [2, 3].

To improve the efficiency of engineering skeletal muscle, a number of key properties of the scaffolds need to be optimized, including conductivity, degradability, and ductility. Conducting scaffolds are attractive for skeletal muscle tissue engineering because they not only provide physical support, but also transmit electrical signal [2, 4–7]. Conducting substrates derived from polypyrrole (PPy) [8], HA-CaTiO3 (hydroxyapatite-calcium titanate), [9], polyaniline (PANi) and poly(ε-caprolactone) (PCL) [6] show positive effect in promoting the proliferation, differentiation, and maturation of skeletal muscle tissue in comparison with non-conductive polymeric substrates [2]. However, there are significant challenges in utilizing these conductive materials for muscle regeneration because of their low or non-degradability, poor mechanical properties, poor solubility and poor processability [10–15]. In contrast, aniline oligomers characteristically have good electroactivity, good processing properties and biodegradability [16–22]. In particular, aniline tetramer (AT) possesses a well-defined electroactive structure, good processability, degradability and biocompatibility [23–26]. Thus, copolymerizing AT with biodegradable polymers could potentially achieve both degradability and the conductivity.

Another desirable property of the polymers for skeletal muscle engineering is ductility. Inflexible substrates are often ineffective in supporting myoblast differentiation as the myoblasts spontaneously contract and often detach from stiff substrates when they are near the end of the differentiation process [27, 28]. The degradable and biocompatible polymers such as poly(lactic acid) (PLA) and its copolymers have been widely applied in tissue engineering. Nevertheless, the disadvantages, such as high modulus and low-yield elongation of PLA, limit its application in regenerating the contractile skeletal muscle tissue that requires a mechanical strain similar to that of the native tissue [1]. A few approaches have been taken to modify PLA for skeletal muscle tissue engineering. For example,

copolymerization of lactide with glycolide can form PLGA polymers with improved properties [29]. Coating PLA with an extracellular matrix (ECM) gel is another example [30]. However, these techniques do not improve the ductility of the polymer. The development of PLA based biomaterials with suitable ductility in skeletal muscle tissue engineering remains a challenge.

In this work, we synthesized ductile and conductive polylactide copolymers, and demonstrated their potential for skeletal muscle regeneration. Star-shaped polylactide was first chain-extended using hexamethylenediisocyanate to obtain ductile polylactide materials, and they were further copolymerized with conductive aniline tetramer (AT), resulting in ductile and electroactive biodegradable copolymers. The chemical structure, electroactivity, thermal properties, and degradability of these polymers were evaluated. C2C12 myoblast cells were then cultured on these polymers to examine their biocompatibility and their effect on the myogenic differentiation. These conductive, ductile, and biodegradable polylactide copolymers significantly enhanced the proliferation and differentiation of C2C12 cells as evidenced by quantitative analysis of myotube number, length, diameter and maturation index, and gene expression of MyoD and TNNT and Western blotting. Our study strongly suggests that these ductile electroactive copolymers are excellent candidates for skeletal muscle regeneration.

2. Experimental section

2.1 Materials

L-lactide (LA) was purified by recrystallization in dry toluene and subsequently dried under reduced pressure (10^{-2} mbar) at room temperature for 48 h prior to polymerization. Aniline (J&K Scientific Ltd.) was distilled twice under reduced pressure. Stannous octoate [$Sn(Oct)_2$, 95%] from Aldrich was dried over molecular sieves and stored at a N_2 atmosphere before use. Pentaerythritol, p-phenylenediamine, camphorsulfonic acid (CSA), phenylhydrazine, succinic anhydride, ammonium persulfate, N-methyl-pyrrolidome (NMP), dichloromethane, 4-dimethylaminopyridine (DMAP), N,N′-dicyclohexyl carbodiimide (DCC), dimethyl sulphoxide (DMSO), dimethylformamide (DMF), chloroform, methanol, ethanol, diethyl ether, hexamethylenediisocyanate (HDI), toluene, anhydrous tetrahydrofuran (THF), phosphate buffer solution (PBS), hexane and HCl were purchased from Aldrich or J&K Scientific Ltd., and were used as received without further purification. Thermomyces lanuginosa was purchased from Sigma. Aniline tetramer (AT) was synthesized according to our previous report [19].

2.2 Synthesis of four-armed PLA and hyperbranched PLA

Four-armed PLA was obtained by ring-opening polymerization (ROP) initiated with pentaerythritol. LA (10 g), initiator ($Sn(Oct)_2$) (22.5 μL), and co-initiator pentaerythritol (236.0 mg), were weighed and added into a 50 mL silanized round bottomed flask in a glovebox (MBraunlabstar). The mixture was then immersed in an oil bath at 110 °C for 48 h. After reaction, 20 mL chloroform was added into the flask to dissolve the crude product. Then the solution was precipitated into cold hexane/diethyl ether (v/v = 95:5) mixture. After filtration, the product was dried in a vacuum oven for 48 h at room temperature.

To synthesize the hyperbranched PLA, the star-shaped PLA, $Sn(Oct)_2$ and HDI were dissolved in anhydrous THF. The matrix was kept at 75 °C in oil bath for 4 h, and precipitated in hexane/diethyl ether (v/v = 95:5) mixture solution. The purified product was coded as HPLA.

2.3 Synthesis of electroactive hyperbranched polylactide copolymers

The synthesis of electroactive hyperbranched PLA copolymers was conducted by an esterification reaction between hydroxyl group of PLA and carboxyl group of AT, and the copolymers obtained were named as HPLAAT. A typical procedure of synthesis of HPLAAT9 was as following: HPLA (0.546 g) and AT (0.054 g) were dissolved in NMP/THF (v/v = 1:3) mixture completely. DCC (60.0 mg) and DMAP (21.3 mg) were then added to the solution to react at ambient temperature for 72 h with continuous stirring. The resultant solution was centrifuged to remove the solid part before precipitation with hexane/diethyl ether (v/v = 95:5) mixture. After filtration, the product was dried in a vacuum oven under reduced pressure for 48 h at room temperature. The theoretical AT contents in the copolymers were set as 3%, 6%, 9%, and 12% (w/w) and the samples were named as HPLAAT3, HPLAAT6, HPLAAT9 and HPLAAT12, respectively.

2.4 Characterization of synthesized HPLAAT and the intermediates between PLA and HPLAAT

FT-IR spectra of all the polymers were recorded on the Nicolet 6700 FT-IR spectrometer (Thermo Scientific Instrument) in a range of 4000–600 cm^{-1}. The spectra were taken as the average of 32 scans at a resolution of 4 cm^{-1}.

^1H NMR (400 MHz) spectra were recorded at ambient temperature using a Bruker Ascend 400 MHz NMR instrument. All the samples containing AT were tested in THF-d_8 to calculate the AT concentration. $CDCl_3$ was used as the solvent for prepolymers PLA, HPLA and DMSO-d_6 for AT. Molecular weights of the PLA and HPLA were determined by comparing the integrals of methine proton peaks (δ= 5.2 ppm, CH) to the ones next to the terminated hydroxyl group (δ= 4.4 ppm, CH). Molecular weight and polydispersity index (PDI) were determined by gel permeation chromatography (GPC) measurement. GPC experiments were conducted at 40 °C with two Waters Styragel columns (HT2 and HT4), a Waters 1525 pump and a Waters 2414 refractive index detector. GPC measurements were carried out in THF at a flow rate of 1 mL/min. Linear polystyrene (Shodex SM-105) was used as a standard. The results of GPC test were listed in Table 1.

The UV-vis spectra of the undoped and doped AT and HPLAAT9 in DMSO solution were recorded on a UV-vis spectrophotometer (PerkinElmer Lambda 35).

Cyclic voltammogram (CV) of HPLAAT12 copolymer was conducted on a CHI 660D electrochemical system (CH Instruments) at a scanning rate of 10 mV/s. An indium tin oxide (ITO) electrode (working electrode), an Ag/AgCl (reference electrode) electrode and a platinum wire (auxiliary electrode) were employed. The ITO glass electrode was immersed into the HPLAAT12 solution dissolved in THF. HPLAAT12 polymer was coated on ITO after THF was evaporated.

Tensile test was carried out by the MTS Criterion 43 instrument equipped with a 50 N tension sensor. The copolymers were dissolved in $CHCl_3$ to form 5 wt% solution and cast onto a superflat polytetrafluoroethylene plats at room temperature to make films. The tests were conducted at a crosshead rate of 2 mm/min. Average value from three samples and standard derivation (SD) of tensile strength, breaking elongation and modulus were reported.

Thermal gravimetric analysis (TGA) was performed on a Mettler-toledo TGA/DSC thermogravimetric analyzer under a N_2 atmosphere (nitrogen flow rate 30 mL/min). The measurements were performed from 50 to 500 °C at a heating rate of 10 °C/min.

Enzymatic degradation was investigated in the presence of proteinase K as described previously [31–33]. The copolymers were dissolved in chloroform with 5 wt% and dried to make films at room temperature. The films were cut into rectangle shape to keep the similar weight of each sample. The samples were then weighed (m1) and immersed in 5 mL Tris/HCl buffer containing 0.2 mg/mL proteinase and incubated at 37 °C on a shaker with shaking speed of 100 r/min. Sodium azide of 0.02 wt % was added to eliminate the growth of microorganisms. At certain interval time, samples were taken out, dried at 60 °C for 24 h in oven and weighed (m2). Results were shown as mean ± standard deviation (n = 5).

$$\text{Weight percentage}\,(\%)=\mathrm{m2}/\mathrm{m1}*\%\quad(1)$$

2.5 C2C12 cell culture

C2C12 myoblast cells originally obtained from the ATCC (American Type Culture Collection) were cultured in Dulbecco's Modified Eagle Medium (DMEM, GIBCO) supplemented with 10% fetal bovine serum (FBS, GIBCO) and 100 U/mL penicillin and 100 U/mL streptomycin, in an incubator at 37 °C in 5% CO_2. When cell confluence reached 90%, cells were passaged as 1:4 by digestion with 0.25 % trypsin. In order to differentiate into myocytes, C2C12 cells were treated with differentiation medium for 7 days which contained 2% horse serum.

2.6 Cell proliferation assay

The samples for cell culture were prepared as described in the literature [20, 34]. The copolymers doped with camphorsulfonic acid (CSA) were dissolved in chloroform to form 1 wt % solutions. The solutions were casted on cover slide with diameter of 18 mm or 22 mm and the solvent was removed by drying at room temperature for 48 h in vacuum.

To investigate the biocompatibility of the materials, C2C12 cells were seeded on the films of HPLA, HPLAAT3, HPLAAT6, HPLAAT9 and HPLAAT12. After sterilized by UV light, films of each sample were fixed in bottom of 24 well plates, and C2C12 cells were seeded on those films at a density of 6000 cells/cm^2. The proliferation rate of cells on the substrates was evaluated by Alamar blue® assay (Molecular Probes) after cultured for 1, 2 and 3 days, respectively [35]. At each point of detection, the cells were incubated in medium containing 10% (v/v) Alamar blue dye at 37 °C in 5% CO_2 for 4 h, then 100 μL medium from each

example was read at 530/600 nm in a SpectraMax fluorescence microplate reader (Molecular Devices). Medium containing 10% (v/v) Alamar blue dye served as blank.

To visualize the cell viability, C2C12 cells on each films were washed with phosphate buffered saline (PBS) three times and treated with Ethidium homodimer-1 (0.5 μM) and calcein AM (0.25 μM) (Live/Dead viability kit, Molecular Probes) for 45 min after cultured for 24 h. Cells were observed under an inverted fluorescent microscope (IX53, Olympus).

2.7 Cell differentiation study

After seeding C2C12 cells on the films 24 h later, the culture medium was replaced with differentiation medium (DMEM + 2% horse serum) and the cells were continued to culture for 7 days. Differentiation medium was renewed every two days.

The total RNA of each sample was extracted using Trizol (Invitrogen) following the manufacturer's instructions. 1 μg RNA was used to synthesize cDNA using a reverse transcription reagent kit (Takara). The real-time PCR was carried out according to the protocol and conducted with an Applied Biosystems 7500 Fast Real-time PCR system with the following temperature profile: 95 °C for 30 s, then 40 cycles of 95 °C for 15 s followed by 1 min at 60 °C. Two different myogenic genes were used to assess the myogenic differentiation: MyoD and Troponin T (TNNT) along with the housekeeping gene gluteraldehyde phosphate dehydrogenase (GAPDH). Primers were purchased from GeneCopoeia and already proved for quantitative real-time PCR. The gene expression was normalized to the housekeeping gene GAPDH in the same sample.

To visualize the myogenic differentiation of C2C12 cells on the films, immunofluorescence staining was performed. Briefly, cells on each film were rinsed with PBS, and fixed with 2.5% gluteraldehyde for 15 min, followed by three times PBS washing, and then treated with 0.3% Triton X-100 for 0.5 h and 1% BSA in PBS for 1 h. Mouse anti-TUBULIN monoclonal antibody (sigma) was diluted at 1:500 and incubated at 4 °C overnight. After being washed for three times with PBS, Alexa flour 488 conjugated secondary antibody (Molecular Probes) was added and incubated for 2 h at room temperature. After three times PBS washing, cells were counterstained with DAPI for 10 min, and observed under an inverted fluorescence microscopy (IX53, Olympus). Three images of each group were taken by using AxioVision software (Carl Zeiss) to obtain the myotube number, myotube length, myotube diameter and maturation index data.

Western blotting was performed after differentiating C2C12 cells on HPLA and HPLAAT6 for 7 days. The cells were washed with PBS and lysed with lysis buffer containing protease inhibitors (TianGen, China). The total protein concentration was determined by the BCA assay (Bio-rad). Protein extracts were heat denatured at 100 °C for 5 min, electrophoretically separated on a 12% SDS-PAGE (Bio-Rad), and then transferred to a PVDF membrane (Millipore). The membrane was blocked with 5% nonfat dried milk in TBST buffer (0.1 M Tris-HCl and 0.1% Tween-20, pH 7.5) for 1 h and probed with GAPDH (1:1,000, Santa Cruz), and MYH2 (1:500, Santa Cruz). Horseradish peroxidase-conjugated anti-rabbit was used as a secondary antibody (1:1,000, Jackson Immunoresearch). The detection was performed using the Thermo Scientific Pierce ECL Western blotting substrate (Thermo

Scientific). The images were scanned by Tanon- 410 automatic gel imaging system (Shanghai Tianneng Corporation, China), and the optical density was determined using Image J software (NIH).

2.8 Statistic analyses

All the data were expressed as mean ± standard deviation. The statistical significance was analyzed by student t-test. Differences were considered statistically significant when $p < 0.05$.

3. Results and discussion

Synthesis of ductile electroactive copolymers

To obtain ductile and electroactive copolymers that are potentially better suited for skeletal muscle tissue regeneration, we synthesized four-armed PLA using a ring-opening polymerization, and then hyperbranched PLA via a chain extension reaction (Figure 1). Next an esterification reaction between hydroxyl group of PLA and carboxyl group of AT were carried out, resulting in electroactive and hyperbranched copolymers named as HPLAAT.

FT-IR spectroscopy was used to verify the chemical structure of the copolymers. After chain extension of PLA, a new peak of HPLA appeared at 1521 cm^{-1} which corresponded to the characteristic stretching vibration combined with out-of-the plane bending of the –C–N– bond of the urethane group (Figure 2a). No peak appeared at 2280 cm^{-1}, indicating that the HDI was completely converted into urethane in HPLA. The carbonyl groups (–CO–) in carboxyl (–COOH) and amide (–NHCO–) groups in AT were indicated by the bands at 1706 cm^{-1} and 1663 cm^{-1} (Figure 2a) and the vibration of the quinoid rings and benzene rings of AT were indicated by the peaks at 1567 cm^{-1} and 1488 cm^{-1}, respectively. Comparing curves of AT and HPLA with HPLAAT12, the copolymer HPLAAT12 showed bands at 1600 cm^{-1} (quinoid rings) and 1507 cm^{-1} (benzenoid rings) from AT, and bands at 1746 cm^{-1} (–COO–) and 1082 cm^{-1} (–C–O–C–) from PLA, indicating that the AT was successfully grafted on HPLA.

The structure and composition of the prepolymers and copolymers were further confirmed by ^{1}H NMR spectra (shown in Figure 2b). The signals of HPLA at 1.3 ppm and 3.2 ppm were assigned to the hydrogens of methane in HDI. In the ^{1}H NMR spectra of HPLAAT12, there were proton signals between 7.8 and 6.4 ppm (multiplet) which were correlated to the hydrogens in the benzene rings [22]. The peaks appeared at 5.2 and 1.5 ppm were indicative of the protons from –CH– and $–CH_3$ of PLA, confirming that AT was successfully grafted on the HPLA chains. Next, GPC was employed to determine the M_n and polydispersity index (PDI) of copolymers. The M_n of HPLA and HPLAAT of the copolymers increased significantly compared to PLA prepolymer (Table 1), further indicating that the HPLA and HPLAAT were obtained. The AT contents in the copolymers were calculated using NMR and UV spectra. By comparing integrals at 7.8-6.4 ppm from benzene rings and 5.2 ppm from PLA (Figure 2b), the contents of AT in HPLAAT were calculated (Table 2). From the intensity of the peak at 580 nm, the AT contents in the copolymers were quantitatively calculated with concentration-absorption curve of AT as standard (Figure 3a). The data from NMR and UV-Vis tests were close and agreed with the theoretical AT contents in the

copolymers (Table 2), indicating that the HPLAAT copolymers were successfully synthesized.

Electrochemistry of the copolymers

The UV-vis spectrometer was used to record the different state transition of AT and HPLAAT9. As shown in Figure 3a, UV spectra of both undoped AT and HPLAAT9 showed two characteristic peaks at 320 nm and 580 nm, which were correlated to the π–π* transition of the benzene rings and the benzenoid to quinoid excitonic transition, respectively. After doping with HCl, the peak at 580 nm decreased and a new absorption peak appeared at 436 nm along with a slight blue shift of the benzenoid absorption peak (320 nm) to 307 nm for the formation of polarons [22]. The new peak at 799 nm corresponding to the localization of the radical polaron confirmed the generation of emeraldine salts [20].

We next examined the cyclic voltammogram of HPLAAT12 copolymers for their electroactivity (Figure 3b). HPLAAT12 film was fabricated on the ITO glass and doped in DMSO with HCl. The cyclic voltammogram of HPLAAT12 showed two pairs of well-defined reduction/oxidation peaks (0.37 V and 0.60 V), which correlated to the redox process from the “leucoemeraldine” to the “emeraldine” state, and then from the “emeraldine” to the “pernigraniline” state. CV result along with UV-vis spectra demonstrated the good electroactivity of the HPLAAT copolymers.

Mechanical properties of the prepolymer and copolymers

The brittleness of pristine polylactide is another factor that restricts its wide application in tissue engineering. Therefore, we aimed at generating HPLAAT with increased ductility. The mechanical properties of the modified polylactide samples were measured by a tensile tester. The low molecular weight PLA was in a powder state with weak mechanical properties. After chain extension of PLA with HDI, hyperbranched polylactide showed a tremendous increase in the elongation at break to 158.9%, which was much higher than other reported modified materials based on PLA with an elongation to failure no more than 24% [35–39]. This is because the HPLA was in an amorphous state due to the chain extension as indicated by DSC analysis as shown in Figure S1. The amorphous state greatly increased the chain mobility of the polylactide, resulting in the ductility of the material. When the AT segment was introduced into HPLA, the modulus of the HPLAAT copolymers increased accordingly with the AT content, and the elongation at break of the HPLAAT samples decreased from 158.9% to 42.7%. Still, the elongation at break of the HPLAAT materials was much higher than those of the pure polylactide, which was about 10%. The much higher elongation at break of these HPLAAT would make them better suited for soft tissue engineering applications.

Degradation properties of the prepolymer and copolymers

We next examined the thermal stability of the copolymers by TGA. A slight weight loss for all the samples was observed from 100 to 200 °C due to the evaporation of moisture and other solvents trapped in the polymers. PLA thermally degraded completely between 210 to 290 °C. After chain extension, weight loss of HPLA sample happened at lower temperature range from 200 to 280 °C, which indicated a weaker thermal stability than PLA. This was

attributed to the disruption of crystallization of HPLA sample. After introduction of AT segment, all the samples showed a two-stage degradation behavior. For the first stage, HPLAAT thermally degraded between 250 and 320 °C, indicating a higher thermal stability than HPLA and PLA. The second stage of degradation started from 320 °C to 330 °C, correlated to the AT segment degradation in HPLAAT. The higher AT content in HPLAAT copolymer showed a higher degradation temperature, and more weight remained because of the good thermal stability of the AT segments.

More importantly, we examined the enzymatic degradation profiles of HPLA and HPLAAT6 (Figure 4b), which is more relevant to their natural degradation after transplantation in vivo. HPLA showed the faster degradation than HPLAAT copolymers probably due to the end hydroxyl group of PLA arms, which play a important role in PLA degradation [21, 40]. HPLAAT3 retained 78% and 55% mass at 24 h and 72 h, respectively. The addition of aniline tetramer (AT) slowed down the degradation process of the HPLAAT copolymer. As the content of AT increased, HPLAAT6 degraded more slowly than HPLAAT3 in proteinase K solution. HPLAAT9 and HPLAAT12 showed similar degradation behavior to HPLAAT6. The degradability of HPLAAT copolymers provided a favorable property for their in vivo application.

HPLAAT significantly promoted C2C12 cell proliferation

Having identified the ductile, electroactive, and biodegradable features of the HPLAAT, we next applied these polymers to C2C12 cells to examine their effect on the skeletal muscle development. C2C12 is a model cell line that has been widely used to study the skeletal muscle regeneration. We first studied whether HPLAAT could promote cell viability and proliferation. Cell viability was investigated by using Live/Dead viability kit with HPLA as control. After cultivation for 1 day, most of cells on all of these substrates were viable as demonstrated by the Live/Dead staining (Figure 5a–f), which indicated that these HPLAAT materials exhibited good biocompatibility in vitro. The quantified Live/Dead staining results are shown in Figure S3. Together, these data indicate that the cell viability of C2C12 myoblasts on HPLA and HPLAAT was essentially the same as that on TCP.

Furthermore, the cell proliferation behavior was quantitatively investigated by using Alamar blue assay. As shown in Figure 5g, cells cultured on HPLAAT3, HPLAAT6, HPLAAT9 and HPLAAT12 proliferated quicker than those on HPLA after cultivation for one day. On the second day, the cells on all of these HPLAAT substrates showed significantly higher cell numbers than that on HPLA ($P<0.05$), and the materials with the highest AT contents exhibited the highest cell proliferation rate. In addition, all HPLAAT materials maintained significantly higher cell number than HPLA after three days ($P<0.05$). In particular, the cell number on HPLAAT12 was two times higher than that on HPLA ($P<0.01$) and exhibited the highest proliferation rate among all synthesized HPLAAT copolymers. Moreover, the cell number on HPLAAT3 with the lowest AT contents was 1.5 times higher than that on HPLA ($P<0.05$). Proliferation test of C2C12 cells on the films by using CCK-8 method was also carried out (Figure S4) and were generally in agreement with the results by Alamar blue assay. All these results demonstrated that the electroactive HPLAAT copolymers significantly enhanced the C2C12 myoblast proliferation compared to HPLA.

HPLAAT promoted myogenic differentiation

Myogenic differentiation plays a critical role in skeletal muscle regeneration. Considering the good biocompatibility, electroactivity, and ductility of the HPLAAT, we further investigated the influence of those electroactive AT-containing polymers on myogenic differentiation of C2C12 cells *in vitro*. C2C12 cells were seeded on the electroactive ductile polymers and cultured in differentiation medium for 7 days. Immunofluorescence staining and qRT-PCR were then performed to evaluate their myogenic differentiation (Figures 6–8). As shown in Figure 6, much more myotubes (green) were formed on HPLAAT polymers than on HPLA.

Next, the myotube number, diameter, length and maturation index, four widely used parameters, were quantified by morphological analysis (Figure 7a–d). Again, much higher numbers of myotubes were formed on the HPLAAT3, HPLAAT6, HPLAAT9 and HPLAAT12 substrates than on HPLA ($P<0.01$). The increase of myotube formation also positively correlated with the AT contents in the copolymers. The lengths of myotubes on the HPLAAT3, HPLAAT6, HPLAAT9 and HPLAAT12 were 403.2, 598.4, 635.9, and 736.7 μm, respectively, which were much longer than those on HPLA (232.3 μm) (Figure 7b), as well as those on polycaprolactone (PCL)/PANi, and poly(L-lactide-co-3-caprolactone)/PANi nanofibers in the literature [41]. The lengths of myotubes were typically 1.7–3.2 folds higher on the HPLAAT than on HPLA, which demonstrated again the positive correlation between the increase of myotube length and AT contents. These results were also consistent with other reports about myogenic differentiation on conductive substrates [6, 9, 41, 42]. The diameters of myotubes were also measured to further quantify myotube formation on these polymer substrates. The diameters of myotubes were 32.5, 39.9, 60.3, 35.0 and 33.6 μm on HPLA, HPLAAT3, HPLAAT6, HPLAAT9 and HPLAAT12, respectively (Figure 7c), which were greater than those on the PCL/PANi nanofiber (no more than 18 μm) [42]. In contrast to myotube length, the effect of AT content in the copolymers on myotube diameter was more complicated. While others reported a linear correlation between substrate electroactivity and myotube diameter [42], the myotubes on the HPLAAT6 with the intermediate AT content had the greatest diameter among the synthesized AT-containing copolymers. This may be because AT range in the copolymers was significantly broader (0–12% (w/w)) in the current study than those in the literature (PANi content of 0–1.5% (w/w)).

Next, the myotube maturation was quantified by determining the ratio of myotube number with more than 5 nuclei to the total myotube number (myotube maturation index). The myotube maturation index of AT-containing materials was approximately 1.93–2.50 folds more than that of HPLA ($P<0.01$), and almost 96.3% of myotubes on the HPLAAT12 were considered to be mature (Figure 7d).

Finally, to investigate the effect of these materials on myogenesis, the myogenic marker gene expression levels were quantified using real-time PCR analysis. MyoD and TNNT, the early and late markers of myogenesis, were used to determine the myogenic differentiation on those substrates. There was no significant difference in the MyoD gene expression level between electroactive copolymers and HPLA at the first day of differentiation (Figure S5).

At the third day, the MyoD gene expressions of all groups increased. Among them the gene expression on HPLAAT6 has increased almost 4 times, whereas the gene expressions on HPLA and HPLAAT3 increased moderately for about 1.3 – 2 times. At the seventh day of differentiation, the MyoD gene expression levels of all groups decreased, compared to those at the third day. The expressions of MyoD on HPLAAT3, HPLAAT6, HPLAAT9 and HPLAAT12 were 1.4, 3.0, 3.3 and 3.2 folds higher than those on HPLA respectively (Figure 8a). The differences were statistically significant ($P<0.05$). In conclusion, these data show that the MyoD gene expression levels on electroactive copolymers were significantly higher than that on HPLA. Similarly, the expression of TNNT on the AT-containing copolymers was also significantly higher than that on HPLA ($P<0.01$) with an exception of HPLAAT3 (Figure 8b).

Cell density may affect differentiation since C2C12 cells have a higher tendency to differentiate at high confluence than at low confluence. To verify whether the higher cell density (faster cell growth on HPLAAT films than HPLA) or the inherent properties of the films enhanced the differentiation, we seeded C2C12 cells on HPLA films with two different densities (6000 cells/cm^2 and 10200 cells/cm^2) to differentiate for 7 days, with cells on HPLAAT6 at 6000 cells/cm^2 serving as the control. We then performed gene expression analyses of MYH2 (Figure S6). There was no significant difference between HPLA with 6000 cells/cm^2 and HPLA with 10200 cells/cm^2 ($P>0.05$), whereas the MYH2 gene expression on HPLAAT6 with was significantly higher than that on HPLA when both had 6000 cells/cm^2 ($P<0.05$). These results indicated that it was AT component (not the cell density in the range studied) that contributed to the enhanced myogenic differentiation of the HPLAAT materials.

Furthermore, the protein level of MYH2, a key marker of myogenic differentiation, was analyzed for the HPLA group and HPLAAT6 group by Western blotting (Figure 8d). After 7 days of myogenic differentiation, the MYH2 protein level on HPLAAT6 film was over 9 times that at the first day, while the MYH2 protein level on HPLA film was 2 times that at the first day. The protein quantification agreed with the immunofluorescence staining results, demonstrating that the AT component in HPLAAT can promote myogenic differentiation of C2C12 cells.

Taken together, the myotube formation of C2C12 cells was greatly enhanced by electroactive substrates, and the AT component significantly improved the myotube diameter, number, length, myotube maturation index, and myogenic marker expression at both mRNA and protein levels. In conclusion, the myogenic differentiation study indicated that these electroactive materials had significantly positive effect on promoting myogenesis and holds great potential in skeletal muscle regeneration.

Conclusions

A series of ductile and conductive degradable copolymers (HPLAAT) based on star-shaped lactide (PLA) and aniline tetramer (AT) was successfully synthesized. These new polymers significantly enhanced the myogenic differentiation of C2C12 myoblasts. These copolymers have tunable modulus, elongation at break, and thermal stability. They showed strain at

break from 158.9% to 42.7% and modulus from 256.2 to 758.2 MPa, which overcomes the brittleness of pristine PLA. The biodegradability of HPLAAT copolymers should be more suitable as scaffolding materials for in vivo muscle tissue engineering application. All the AT-containing copolymers are electroactive and more biocompatible than HPLA without AT. Importantly, the HPLAAT copolymers greatly promoted myogenic differentiation of C2C12 cells as evidenced by quantitative analysis of myotube number, myotube length, myotube diameter, maturation index, and myogenic gene expression. We expect that these electroactive ductile polylactide copolymers will serve as excellent scaffolds in tissue engineering to regenerate skeletal muscle and possibly other tissues.

Supplementary Material

Refer to Web version on PubMed Central for supplementary material.

Acknowledgments

The authors would like to gratefully acknowledge the financial support for this work from the National Natural Science Foundation of China (grant number: 21304073) and the National Institutes of Health of the US (NHLBI HL114038: PXM & YEC).

References

1. Riboldi SA, Sampaolesi M, Neuenschwander P, Cossu G, Mantero S. Electrospun degradable polyesterurethane membranes: potential scaffolds for skeletal muscle tissue engineering. Biomaterials. 2005; 26:4606–15. [PubMed: 15722130]
2. Gilmore KJ, Kita M, Han Y, Gelmi A, Higgins MJ, Moulton SE, Clark GM, Kapsa R, Wallace GG. Skeletal muscle cell proliferation and differentiation on polypyrrole substrates doped with extracellular matrix components. Biomaterials. 2009; 30:5292–304. [PubMed: 19643473]
3. Bach A, Beier J, Stern-Staeter J, Horch R. Skeletal muscle tissue engineering. Journal of cellular and molecular medicine. 2004; 8:413–22. [PubMed: 15601570]
4. Guimard NK, Gomez N, Schmidt CE. Conducting polymers in biomedical engineering. Progress in Polymer Science. 2007; 32:876–921.
5. Jun I, Jeong S, Shin H. The stimulation of myoblast differentiation by electrically conductive sub-micron fibers. Biomaterials. 2009; 30:2038–47. [PubMed: 19147222]
6. Chen MC, Sun YC, Chen YH. Electrically conductive nanofibers with highly oriented structures and their potential application in skeletal muscle tissue engineering. Acta Biomater. 2013; 9:5562–72. [PubMed: 23099301]
7. Li L, Ge J, Guo B, Ma PX. In situ forming biodegradable electroactive hydrogels. Polym Chem. 2014; 5:2880–90.
8. Rowlands AS, Cooper-White JJ. Directing phenotype of vascular smooth muscle cells using electrically stimulated conducting polymer. Biomaterials. 2008; 29:4510–20. [PubMed: 18789820]
9. Thrivikraman G, Mallik PK, Basu B. Substrate conductivity dependent modulation of cell proliferation and differentiation in vitro. Biomaterials. 2013; 34:7073–85. [PubMed: 23796580]
10. Hu J, Huang L, Zhuang X, Zhang P, Lang L, Chen X, Wei Y, Jing X. Electroactive aniline pentamer cross-linking chitosan for stimulation growth of electrically sensitive cells. Biomacromolecules. 2008; 9:2637–44. [PubMed: 18698845]
11. Ghasemi-Mobarakeh L, Prabhakaran MP, Morshed M, Nasr-Esfahani MH, Ramakrishna S. Electrical stimulation of nerve cells using conductive nanofibrous scaffolds for nerve tissue engineering. Tissue Eng Part A. 2009; 15:3605–19. [PubMed: 19496678]
12. Xie J, MacEwan MR, Willerth SM, Li X, Moran DW, Sakiyama-Elbert SE, Xia Y. Conductive core– sheath nanofibers and their potential application in neural tissue engineering. Advanced functional materials. 2009; 19:2312–8. [PubMed: 19830261]

13. Guo B, Glavas L, Albertsson A-C. Biodegradable and electrically conducting polymers for biomedical applications. Progress in polymer science. 2013; 38:1263–86.
14. Guo B, Finne-Wistrand A, Albertsson A-C. Simple route to size-tunable degradable and electroactive nanoparticles from the self-assembly of conducting coil–rod–coil triblock copolymers. Chemistry of Materials. 2011; 23:4045–55.
15. Guo B, Finne-Wistrand A, Albertsson A-C. Electroactive hydrophilic polylactide surface by covalent modification with tetraaniline. Macromolecules. 2012; 45:652–9.
16. Guo B, Finne-Wistrand A, Albertsson A-C. Molecular architecture of electroactive and biodegradable copolymers composed of polylactide and carboxyl-capped aniline trimer. Biomacromolecules. 2010; 11:855–63. [PubMed: 20201489]
17. Cui H, Shao J, Wang Y, Zhang P, Chen X, Wei Y. PLA-PEG-PLA and its electroactive tetraaniline copolymer as multi-interactive injectable hydrogels for tissue engineering. Biomacromolecules. 2013; 14:1904–12. [PubMed: 23611017]
18. Guo B, Finne-Wistrand A, Albertsson A-C. Enhanced electrical conductivity by macromolecular architecture: Hyperbranched electroactive and degradable block copolymers based on poly (ε-caprolactone) and aniline pentamer. Macromolecules. 2010; 43:4472–80.
19. Ma X, Ge J, Li Y, Guo B, Ma PX. Nanofibrous electroactive scaffolds from a chitosan-grafted-aniline tetramer by electrospinning for tissue engineering. RSC Advances. 2014; 4:13652–61.
20. Huang L, Hu J, Lang L, Wang X, Zhang P, Jing X, Wang X, Chen X, Lelkes PI, MacDiarmid AG. Synthesis and characterization of electroactive and biodegradable ABA block copolymer of polylactide and aniline pentamer. Biomaterials. 2007; 28:1741–51. [PubMed: 17218007]
21. Huang L, Zhuang X, Hu J, Lang L, Zhang P, Wang Y, Chen X, Wei Y, Jing X. Synthesis of biodegradable and electroactive multiblock polylactide and aniline pentamer copolymer for tissue engineering applications. Biomacromolecules. 2008; 9:850–8. [PubMed: 18260636]
22. Guo B, Finne-Wistrand A, Albertsson A-C. Degradable and electroactive hydrogels with tunable electrical conductivity and swelling behavior. Chemistry of Materials. 2011; 23:1254–62.
23. Lu W, Sheng Meng X, Yuan Wang Z. Electrochemical behavior of a new electroactive polyimide derived from aniline trimer. J Polym Sci Pol Chem. 1999; 37:4295–301.
24. Wang ZY, Yang C, Gao JP, Lin J, Meng X, Wei Y, Li S. Electroactive polyimides derived from amino-terminated aniline trimer. Macromolecules. 1998; 31:2702–4.
25. Bidez PR, Li S, MacDiarmid AG, Venancio EC, Wei Y, Lelkes PI. Polyaniline, an electroactive polymer, supports adhesion and proliferation of cardiac myoblasts. J Biomat Sci-Polym E. 2006; 17:199–212.
26. Wang C, Dong Y, Sengothi K, Tan K, Kang E. *In-vivo* tissue response to polyaniline. Synthetic Met. 1999; 102:1313–4.
27. Cooper S, Maxwell A, Kizana E, Ghoddusi M, Hardeman E, Alexander I, Allen D, North K. C2C12 co-culture on a fibroblast substratum enables sustained survival of contractile, highly differentiated myotubes with peripheral nuclei and adult fast myosin expression. Cell motility and the cytoskeleton. 2004; 58:200–11. [PubMed: 15146538]
28. Ren K, Crouzier T, Roy C, Picart C. Polyelectrolyte multilayer films of controlled stiffness modulate myoblast cell differentiation. Advanced functional materials. 2008; 18:1378–89. [PubMed: 18841249]
29. Levenberg S, Rouwkema J, Macdonald M, Garfein ES, Kohane DS, Darland DC, Marini R, van Blitterswijk CA, Mulligan RC, D'Amore PA. Engineering vascularized skeletal muscle tissue. Nature biotechnology. 2005; 23:879–84.
30. Cronin EM, Thurmond FA, Bassel-Duby R, Williams RS, Wright WE, Nelson KD, Garner HR. Protein-coated poly (L-lactic acid) fibers provide a substrate for differentiation of human skeletal muscle cells. Journal of Biomedical Materials Research Part A. 2004; 69:373–81. [PubMed: 15127383]
31. Numata K, Srivastava RK, Finne-Wistrand A, Albertsson A-C, Doi Y, Abe H. Branched poly(lactide) synthesized by enzymatic polymerization: Effects of molecular branches and stereochernistry on enzymatic degradation and alkaline hydrolysis. Biomacromolecules. 2007; 8:3115–25. [PubMed: 17722879]

32. Wang CH, Fan KR, Hsiue GH. Enzymatic degradation of PLLA-PEOz-PLLA triblock copolymers. Biomaterials. 2005; 26:2803–11. [PubMed: 15603776]
33. Tsuji H, Miyauchi S. Enzymatic hydrolysis of poly(lactide)s: Effects of molecular weight, L-lactide content, and enantiomeric and diastereoisomeric polymer blending. Biomacromolecules. 2001; 2:597–604. [PubMed: 11749226]
34. Cui H, Liu Y, Deng M, Pang X, Zhang P, Wang X, Chen X, Wei Y. Synthesis of Biodegradable and Electroactive Tetraaniline Grafted Poly(ester amide) Copolymers for Bone Tissue Engineering. Biomacromolecules. 2012; 13:2881–9. [PubMed: 22909313]
35. Li L, Ge J, Wang L, Guo B, Ma PX. Electroactive nanofibrous biomimetic scaffolds by thermally induced phase separation. Journal of materials Chemistry B. 2014; 2:6119–30.
36. Qingwei Z, Mochalin VN, Neitzel I, Hazeli K, Junjie N, Kontsos A, Zhou JG, Lelkes PI, Gogotsi Y. Mechanical properties and biomineralization of multifunctional nanodiamond-PLLA composites for bone tissue engineering. Biomaterials. 2012; 33:5067–75. [PubMed: 22494891]
37. Renouf-Glauser AC, Rose J, Farrar DF, Cameron RE. The effect of crystallinity on the deformation mechanism and bulk mechanical properties of PLLA. Biomaterials. 2005; 26:5771–82. [PubMed: 15949544]
38. Venkatraman S, Poh TL, Vinalia T, Mak KH, Boey F. Collapse pressures of biodegradable stents. Biomaterials. 2003; 24:2105–11. [PubMed: 12628831]
39. Li Y, Shimizu H. Improvement in toughness of poly (l-lactide)(PLLA) through reactive blending with acrylonitrile–butadiene–styrene copolymer (ABS): morphology and properties. European Polymer Journal. 2009; 45:738–46.
40. Riva R, Schmeits P, Stoffelbach F, Jerome C, Jerome R, Lecomte P. Combination of ring-opening polymerization and “click” chemistry towards functionalization of aliphatic polyesters. Chemical Communications. 2005:5334–6. [PubMed: 16244746]
41. Jun I, Jeong S, Shin H. The stimulation of myoblast differentiation by electrically conductive sub-micron fibers. Biomaterials. 2009; 30:2038–47. [PubMed: 19147222]
42. Ku SH, Lee SH, Park CB. Synergic effects of nanofiber alignment and electroactivity on myoblast differentiation. Biomaterials. 2012; 33:6098–104. [PubMed: 22681977]
43. Wu Y, Wang L, Guo B, Ma PX. Injectable biodegradable hydrogels and microgels based on methacrylated poly (ethylene glycol)-co-poly (glycerol sebacate) multi-block copolymers: synthesis, characterization, and cell encapsulation. Journal of Materials Chemistry B. 2014; 2:3674–85.

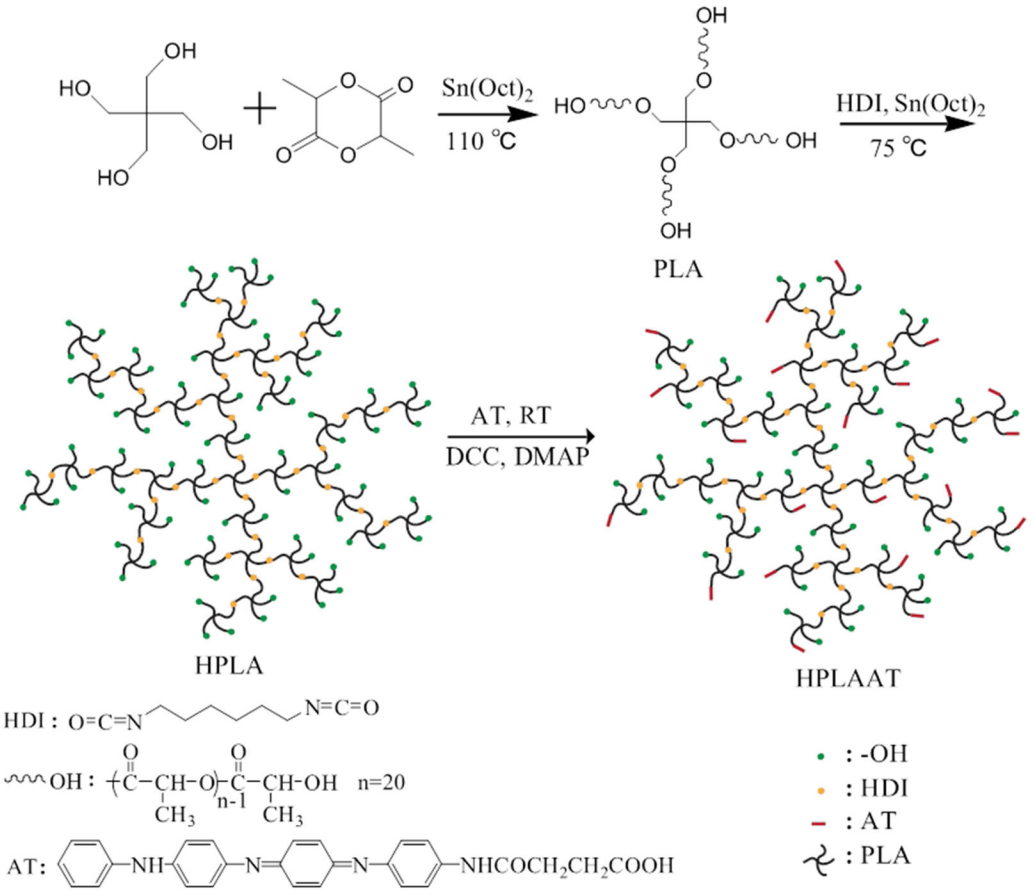

Figure 1.
Schematic synthesis of electroactive hyperbranched HPLAAT.

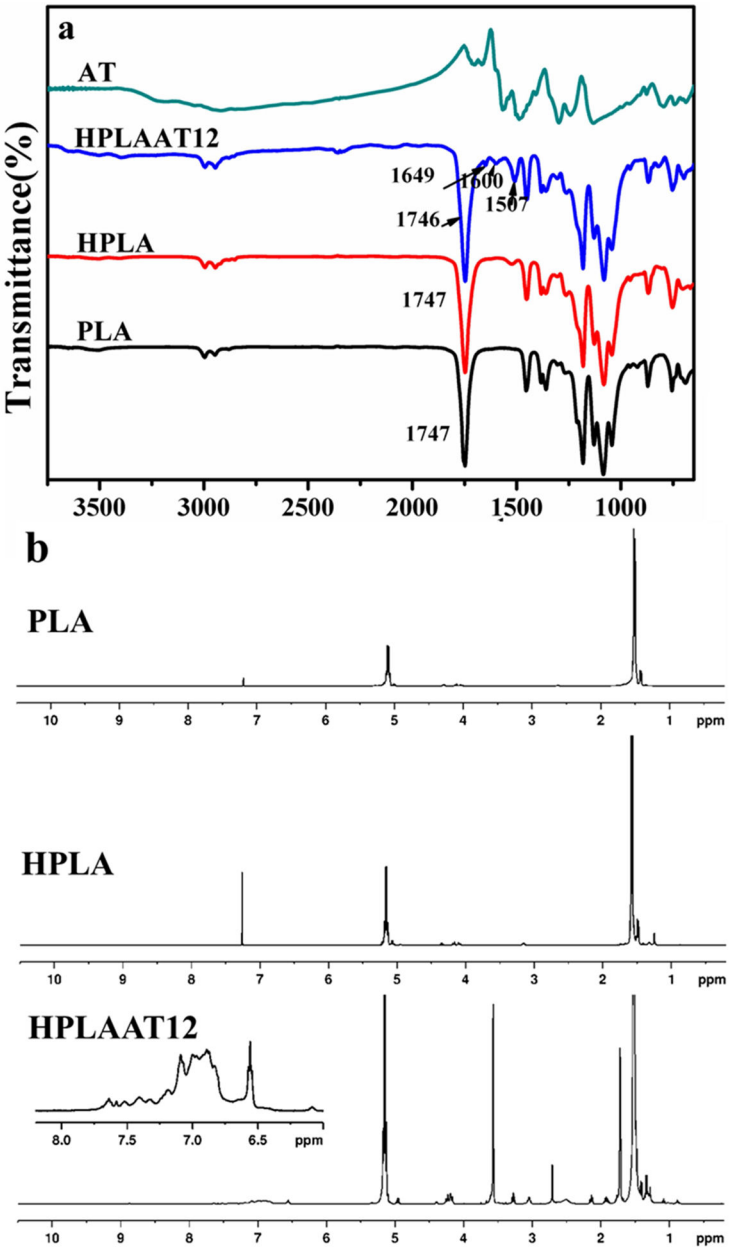

Figure 2.

(a) FT-IR spectra of AT, HPLAAT12, HPLA and PLA; (b) NMR ^{1}H NMR spectra of PLA, HPLA, and HPLAAT12.

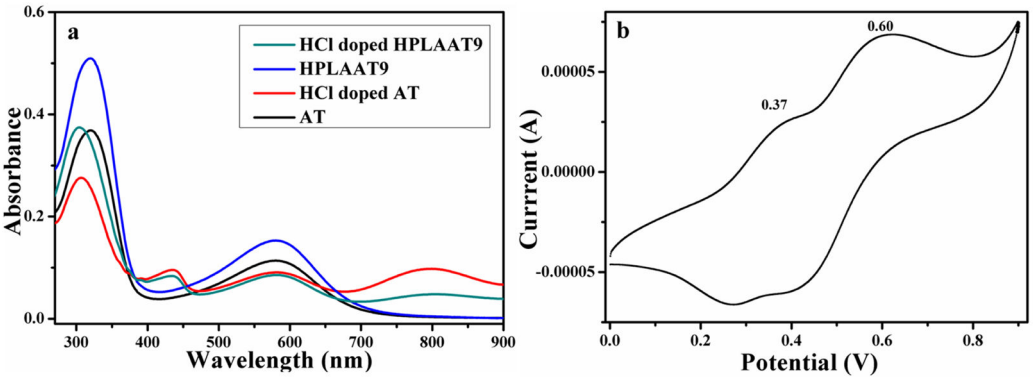

Figure 3.

(a) UV-vis spectra of AT and HPLAAT9 in DMSO; (b) CV curve of HPLAAT12 sample in DMSO.

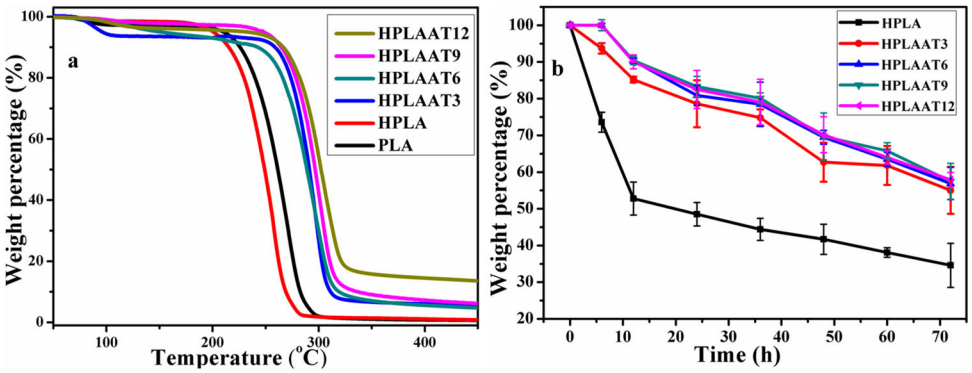

Figure 4.

(a) TGA curves of the PLA, HPLA, and HPLAAT copolymers; (b) Degradation profiles of the HPLA and HPLAAT copolymers

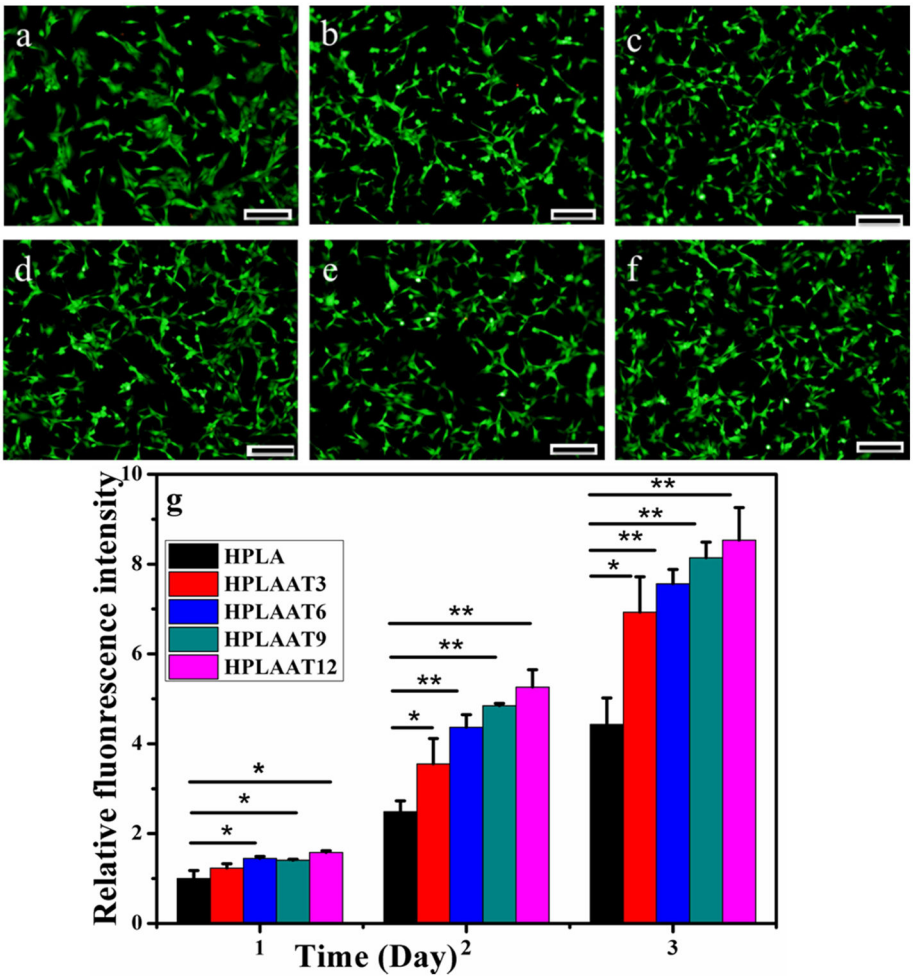

Figure 5.

The viability of C2C12 myoblasts cultured with TCP (a), HPLA (b), HPLAAT3 (c), HPLAAT6 (d), HPLAAT9 (e), or HPLAAT12 (f) after 24 h. A Live/Dead staining kit was applied [43]. The green fluorescence indicated live cells. Scale bar: 200 μm. (g) The proliferation of C2C12 myoblasts cultured on HPLA, HPLAAT3, HPLAAT6, HPLAAT9 and HPLAAT12. Mean for n = 4±SD. * means $P<0.05$. ** means $P<0.01$.

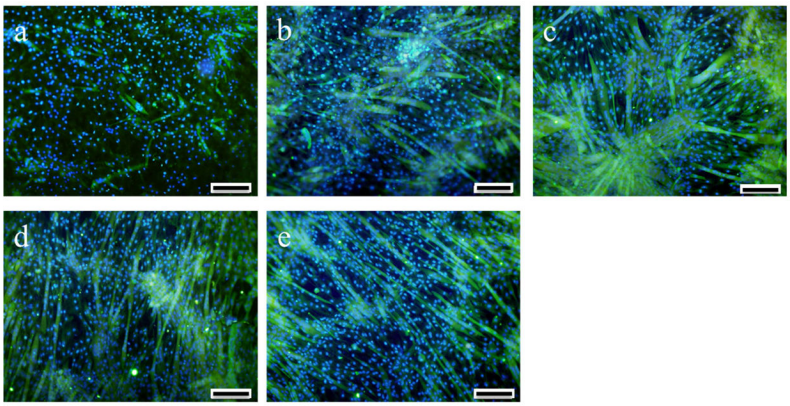

Figure 6.

Tubulin (green) and nuclei (blue) staining of C2C12 cells after 7 days in differentiation medium on HPLA and HPLAAT substrates: (a) HPLA, (b) HPLAAT3, (c) HPLAAT6, (d) HPLAAT9 and (e) HPLAAT12. Scale bar: 200 μm.

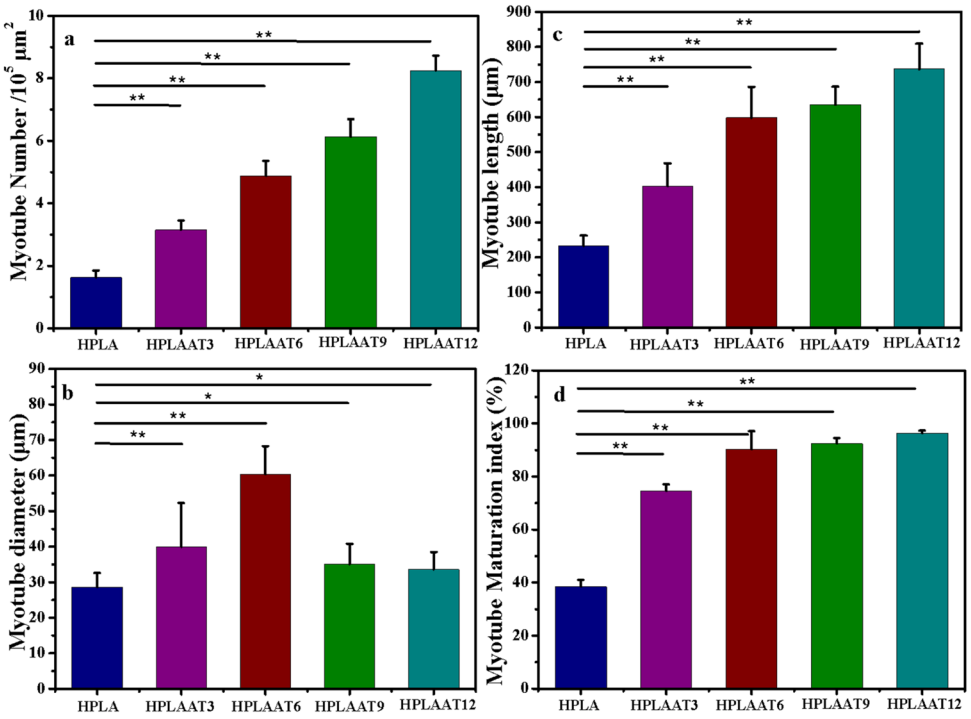

Figure 7.

Quantitative analysis of (a) myotube number per 10^5 μm^2, (b) myotube length, (c) myotube diameter, and (d) myotube maturation index (% myotubes with ≥5 nuclei). Data are presented as Mean ± SD (n = 3). **P*<0.05. ***P*<0.01.

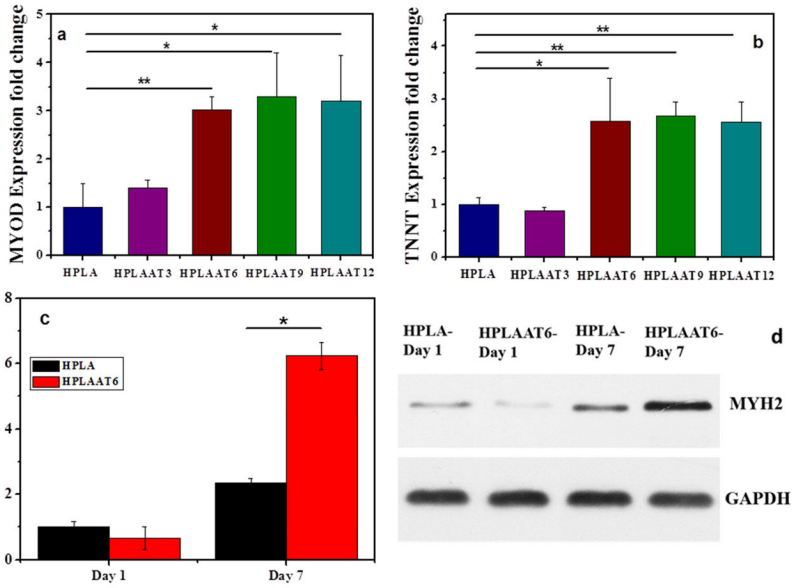

Figure 8.

Myogenic gene expression at day 7 and MYH2 protein levels at days 1 and 7 during differentiation. (a) MyoD gene expression, (b) TNNT gene expression, (c) MYH2 protein levels at days 1 and 7, and (d) the corresponding Western blotting results at days 1 and 7. Mean ± SD (n=3). **P*<0.05. ***P*<0.01.

Table 1

GPC results of the prepolymers and copolymers

Sample name	PLA	HPLA	HPLAAT3	HPLAAT6	HPLAAT9	HPLAAT12
M_n by GPC	8070	35600	42400	42800	37500	37400
PDI	1.2	2.0	1.6	2.6	2.2	1.5

Table 2

Weight ratio of AT in hyperbranched copolymers calculated by NMR and UV

Sample name	HPLAAT3	HPLAAT6	HPLAAT9	HPLAAT12
Theoretical content of AT	3.0%	6.0%	9.0%	12.0%
Weight ratio of AT by NMR	3%	4.5%	6.2%	9.7%
Weight ratio of AT by UV	2.8%	3.5%	5.3%	8.0%

Table 3

Tensile tests of the copolymer films

Sample name	Stress (MPa)	Elongation at break (%)	Modulus (MPa)
HPLA	4.3±0.7	158.9±39.0	265.2±53.4
HPLAAT3	6.5±0.8	109.0±32.8	514.0±78.7
HPLAAT6	8.8±0.7	79.9±11.6	573.1±66.2
HPLAAT9	10.4±0.6	54.9±12.5	749.4±45.8
HPLAAT12	11.6±0.6	42.7±8.8	758.2±10.4